

MEMO No CFD/THERMO-44-2003 DATE: 17th December 2003

TITLE

Test Simulations with the NACA 0012 Airfoil

AUTHOR(S)

Juhaveikko Ala-Juusela

ABSTRACT

Air-flow around the NACA 0012 airfoil was simulated with the FINFLO flow solver version 7.2 of Finflo Ltd. and the 2D solver FINF2D of the Laboratory of Aerodynamics, HUT. The flow conditions are $Ma = 0.3$, $\alpha = 10^\circ$.

MAIN RESULT

Pressure and friction coefficients are in a good agreement between the two solvers, whereas the drag and lift coefficients have some differences.

PAGES

21

KEY WORDS

FINFLO, $k - \omega$ model, $k - \varepsilon$ model, NACA 0012 Airfoil

APPROVED BY

Timo Siikonen 17th December 2003

Contents

1	Introduction	5
2	Flow Equations	5
3	Turbulence Modelling	7
3.1	$k - \varepsilon$ Turbulence Model	7
3.2	$k - \omega$ Turbulence Model	8
4	Computational Grid	10
5	Results	10
6	Discussion	16
A	Convergence histories of the $k - \varepsilon$ turbulence model	18
B	Convergence histories of the $k - \omega$ turbulence model	20

1 Introduction

In this study an air-flow around the NACA 0012 airfoil was simulated numerically with two different flow solver codes/versions, utilizing $k - \varepsilon$ and $k - \omega$ turbulence models. The codes were FINF2D, a two-dimensional flow solver developed in HUT Laboratory of Aerodynamics and FINFLO-7.2 flow solver maintained by Finflo Ltd. The flow conditions are $Ma = 0.3$, $\alpha = 10^\circ$.

The purpose of the present study was to verify the computer codes. The development of the FINF2D code is mainly concentrated into the $k - \omega$ turbulence model and it was considered to be more important in this comparison. In the following the turbulence models are firstly described. Next, the computational grid is depicted and, finally, the results of the simulation are presented and compared.

2 Flow Equations

The Reynolds-averaged Navier-Stokes equations, and the equations for the kinetic energy (k) and dissipation (ϵ) of turbulence can be written in the following form

$$\frac{\partial U}{\partial t} + \frac{\partial(F - F_v)}{\partial x} + \frac{\partial(G - G_v)}{\partial y} + \frac{\partial(H - H_v)}{\partial z} = Q \quad (1)$$

where the unknowns are $U = (\rho, \rho u, \rho v, \rho w, E, \rho k, \rho \epsilon)^T$. The last equation can be replaced by that of ω . The inviscid fluxes are

$$F = \begin{pmatrix} \rho u \\ \rho u^2 + p + \frac{2}{3}\rho k \\ \rho v u \\ \rho w u \\ (E + p + \frac{2}{3}\rho k)u \\ \rho u k \\ \rho u \epsilon \end{pmatrix} \quad G = \begin{pmatrix} \rho v \\ \rho v u \\ \rho v^2 + p + \frac{2}{3}\rho k \\ \rho w v \\ (E + p + \frac{2}{3}\rho k)v \\ \rho v k \\ \rho v \epsilon \end{pmatrix} \quad H = \begin{pmatrix} \rho w \\ \rho w u \\ \rho v w \\ \rho w^2 + p + \frac{2}{3}\rho k \\ (E + p + \frac{2}{3}\rho k)w \\ \rho w k \\ \rho w \epsilon \end{pmatrix} \quad (2)$$

where ρ is the density, the velocity vector by using Cartesian components is $\vec{V} = u\vec{i} + v\vec{j} + w\vec{k}$, p is the pressure, k is the turbulent kinetic energy and ϵ its dissipation, and the total energy E is defined as

$$E = \rho e + \frac{\rho \vec{V} \cdot \vec{V}}{2} + \rho k \quad (3)$$

where e is the specific internal energy. The viscous fluxes are

$$F_v = \begin{pmatrix} 0 \\ \tau_{xx} \\ \tau_{xy} \\ \tau_{xz} \\ u\tau_{xx} + v\tau_{xy} + w\tau_{xz} - q_x \\ \mu_k(\partial k / \partial x) \\ \mu_\epsilon(\partial \epsilon / \partial x) \end{pmatrix} \quad G_v = \begin{pmatrix} 0 \\ \tau_{xy} \\ \tau_{yy} \\ \tau_{yz} \\ u\tau_{xy} + v\tau_{yy} + w\tau_{yz} - q_y \\ \mu_k(\partial k / \partial y) \\ \mu_\epsilon(\partial \epsilon / \partial y) \end{pmatrix}$$

$$H_v = \begin{pmatrix} 0 \\ \tau_{xz} \\ \tau_{yz} \\ \tau_{zz} \\ u\tau_{xz} + v\tau_{yz} + w\tau_{zz} - q_z \\ \mu_k(\partial k/\partial z) \\ \mu_\epsilon(\partial \epsilon/\partial z) \end{pmatrix} \quad (4)$$

Here the stress tensor, τ_{ij} , includes laminar and turbulent components. The fluid is assumed to be Newtonian and, therefore, the laminar stresses are modelled by using Stokes hypothesis. The Reynolds stresses $\overline{\rho u_i'' u_j''}$ are included to the stress tensor τ_{ij} .

$$\tau_{ij} = \mu \left[\frac{\partial u_j}{\partial x_i} + \frac{\partial u_i}{\partial x_j} - \frac{2}{3}(\nabla \cdot \vec{V})\delta_{ij} \right] - \overline{\rho u_i'' u_j''} + \frac{2}{3}\rho k\delta_{ij} \quad (5)$$

For the Reynolds stresses the Boussinesq's approximation

$$-\overline{\rho u_i'' u_j''} = \mu_T \left[\frac{\partial u_j}{\partial x_i} + \frac{\partial u_i}{\partial x_j} - \frac{2}{3}(\nabla \cdot \vec{V})\delta_{ij} \right] - \frac{2}{3}\rho k\delta_{ij} \quad (6)$$

is utilized. Here μ_T is a turbulent viscosity coefficient, which is calculated by using a turbulence model, and δ_{ij} is the Kronecker's delta. In the momentum and energy equations, the kinetic energy contribution $2/3\rho k\delta_{ij}$ has been connected with pressure and appears in the convective fluxes, whereas the diffusive part is connected with the viscous fluxes. The viscous stresses contains a laminar and a turbulent part. Respectively, the heat flux can be written as

$$\vec{q} = -(\lambda + \lambda_T)\nabla T = -\left(\mu \frac{c_p}{Pr} + \mu_T \frac{c_p}{Pr_T}\right)\nabla T \quad (7)$$

where λ is a molecular and λ_T a turbulent thermal conductivity coefficient and Pr is a laminar and Pr_T a turbulent Prandtl number, respectively, and c_p is a specific heat at constant pressure. The diffusion of turbulence variables is modelled as

$$\mu_k \nabla k = \left(\mu + \frac{\mu_T}{\sigma_k}\right)\nabla k \quad (8)$$

$$\mu_\epsilon \nabla \epsilon = \left(\mu + \frac{\mu_T}{\sigma_\epsilon}\right)\nabla \epsilon \quad (9)$$

where σ_k and σ_ϵ are turbulent Schmidt's number of k and ϵ , respectively. The pressure is calculated from an equation of state $p = p(\rho, e)$, which, with a perfect gas assumption utilized in this study, is written as

$$p = (\gamma - 1)\left(E - \frac{\rho \vec{V} \cdot \vec{V}}{2} - \rho k\right) = (\gamma - 1)\rho e \quad (10)$$

where γ is the ratio of specific heats c_p/c_v . Since this case is essentially incompressible, pressure differences are solved instead of pressure. The components of the source term Q are non-zero in turbulence model equations.

3 Turbulence Modelling

3.1 $k - \epsilon$ Turbulence Model

As mentioned, turbulent stresses resulting from the Reynolds averaging of the momentum equation are modelled by using Boussinesq's approximation (6). The turbulent viscosity coefficient μ_T is determined by using Chien's [1] low-Reynolds number $k - \epsilon$ model from the formula

$$\mu_T = c_\mu \rho \frac{k^2}{\epsilon} \quad (11)$$

where c_μ is a empirical coefficient. The source term of Chien's model is

$$Q = \begin{pmatrix} P - \rho\epsilon - 2\mu \frac{k}{y_n^2} \\ c_1 \frac{\epsilon}{k} P - c_2 \frac{\rho\epsilon^2}{k} - 2\mu \frac{\epsilon}{y_n^2} e^{-y^+/2} \end{pmatrix} \quad (12)$$

where y_n is the normal distance from the wall, and the dimensionless distance y^+ is defined by

$$y^+ = y_n \frac{\rho u_\tau}{\mu} = y_n \frac{\sqrt{\rho \tau_w}}{\mu} \approx y_n \left[\frac{\rho |\nabla \times \vec{V}|}{\mu} \right]_w^{1/2} \quad (13)$$

Here u_τ is friction velocity and τ_w is friction on the wall, and the connection between them is $u_\tau = \sqrt{\tau_w/\rho}$. The unknown production of the turbulent kinetic energy is modelled using Boussinesq's approximation (6)

$$\begin{aligned} P &= -\overline{\rho u_i'' u_j''} \frac{\partial u_i}{\partial x_j} \\ &= \left[\mu_T \left(\frac{\partial u_i}{\partial x_j} + \frac{\partial u_j}{\partial x_i} - \frac{2}{3} \delta_{ij} \frac{\partial u_k}{\partial x_k} \right) - \frac{2}{3} \delta_{ij} \rho k \right] \frac{\partial u_i}{\partial x_j} \end{aligned} \quad (14)$$

The turbulence model presented above contains empirical coefficients. Those are given by [2]

$$\begin{aligned} c_1 &= 1.44 & \sigma_k &= 1.0 \\ c_2 &= 1.92(1 - 0.22e^{-Re_T^2/36}) & \sigma_\epsilon &= 1.3 \\ c_\mu &= 0.09(1 - e^{-0.0115y^+}) \end{aligned} \quad (15)$$

where the turbulence Reynolds number is defined as

$$Re_T = \frac{\rho k^2}{\mu \epsilon} \quad (16)$$

Chien's model is very robust, but it has several shortcomings. It usually overestimates the turbulence level and is not performing well in a case of an increasing pressure gradient.

3.2 $k - \omega$ Turbulence Model

In order to improve the near-wall behaviour of a $k - \varepsilon$ model, a mixture of the $k - \varepsilon$ and $k - \omega$ models, known as Menter's $k - \omega$ SST model [3, 4, 5], has gained increasing popularity in recent years. The development of the FINF2D code is mainly concentrated into this model and it was considered to be more important in this comparison.

Menter's $k - \omega$ SST -model is a two-equation turbulence model where the $k - \omega$ -model is utilized in a boundary layer and outside of that the turbulence is modelled with the $k - \varepsilon$ -model. However, the ε -equation is transferred into the ω -equation in order to allow a smooth change between the models. In the SST-model the turbulent stress is limited in a boundary layer in order to avoid unrealistic strain-rates, which are typical to the Boussinesq eddy viscosity models. The equations for k and ω are

$$\rho \frac{\partial k}{\partial t} + \rho u_j \frac{\partial k}{\partial x_j} = P - \beta^* \rho k \omega \quad (17)$$

$$+ \frac{\partial}{\partial x_j} \left[\left(\mu + \frac{\mu_T}{\sigma_k} \right) \frac{\partial k}{\partial x_j} \right]$$

$$\rho \frac{\partial \omega}{\partial t} + \rho u_j \frac{\partial \omega}{\partial x_j} = \frac{\gamma \rho}{\mu_T} P \quad (18)$$

$$+ \frac{\partial}{\partial x_j} \left[\left(\mu + \frac{\mu_T}{\sigma_\omega} \right) \frac{\partial \omega}{\partial x_j} \right]$$

$$+ 2\rho \frac{1 - F_1}{\sigma_{\omega 2} \omega} \frac{\partial k}{\partial x_j} \frac{\partial \omega}{\partial x_j}$$

The model coefficients in Eqs. (17) and (18) are obtained from

$$(\sigma_k \ \sigma_\omega \ \beta)^T = F_1 (\sigma_k \ \sigma_\omega \ \beta)_1^T + (1 - F_1) (\sigma_k \ \sigma_\omega \ \beta)_2^T \quad (19)$$

with the following values

$$\begin{array}{lll} \sigma_{k1} = 1.176 & \sigma_{\omega 1} = 2.0 & \beta_1 = 0.075 \\ \sigma_{k2} = 1.0 & \sigma_{\omega 2} = 1.168 & \beta_2 = 0.0828 \end{array}$$

Coefficients κ and β^* have constant values 0.41 and 0.09. Coefficient γ is calculated from

$$\gamma = \frac{\beta}{\beta^*} - \frac{\kappa^2}{\sigma_\omega \sqrt{\beta^*}} \quad (20)$$

Term P in Eqs. (17) and (18) is a production of the turbulent kinetic energy and it is calculated from Eq. (14). The last term in the ω -equation originates from the transformed ε -equation and it is called a cross-diffusion term. The switching function which governs the choice between the ω - and the ε -equations is

$$F_1 = \tanh(\Gamma^4) \quad (21)$$

where

$$\Gamma = \min \left(\max \left(\frac{\sqrt{k}}{\beta^* \omega d}; \frac{500\nu}{\omega d^2} \right); \frac{4\rho\sigma_{\omega 2}k}{CD_{k\omega}d^2} \right) \quad (22)$$

The first term is turbulent length scale divided with the distance from the walls. This ratio is around 2.5 in a logarithmic layer and approach zero in a outer layer. The second term has a value of ≥ 1 only in a viscous sublayer. The meaning of the third term is to ensure stable behaviour of F_1 when the value of ω in the free stream is small. $CD_{k\omega}$ is the positive part of the cross diffusion term

$$CD_{k\omega} = \max \left(\frac{2\rho}{\sigma_{\omega 2}\omega} \frac{\partial k}{\partial x_j} \frac{\partial \omega}{\partial x_j}; CD_{k\omega \min} \right) \quad (23)$$

where $CD_{k\omega \min}$ is a specified lower limit of the cross diffusion term.

In the original SST-model the eddy viscosity μ_T is defined as

$$\mu_T = \frac{a_1 \rho k}{\max(a_1 \omega; |\Omega_{ij}| F_2 F_3)} \quad (24)$$

where $a_1 = 0.31$ and $|\Omega_{ij}| = \sqrt{2\Omega_{ij}\Omega_{ij}}$, with Ω_{ij} being the vorticity tensor

$$\Omega_{ij} = \frac{1}{2} \left(\frac{\partial u_i}{\partial x_j} - \frac{\partial u_j}{\partial x_i} \right) \quad (25)$$

Above term F_2 is a switching function that disables the SST limitation outside of the boundary layers. Function F_2 works like function F_1 except its value remains as one farther in the outer boundary layer. It is defined as

$$F_2 = \tanh(\Gamma_2^2) \quad (26)$$

where

$$\Gamma_2 = \max \left(\frac{2\sqrt{k}}{\beta^* \omega d}; \frac{500\nu}{\omega d^2} \right) \quad (27)$$

In Eq. (24) the lower limit of the nominator is based on Bradshaw's assumption, on which the turbulent shear stress in the boundary layer depends on k as follows:

$$|\overline{\rho u'' v''}| = a_1 \rho k \quad (28)$$

Thus the traditional Kolmogorov-Prandtl-expression $\mu_T = \rho k / \omega$ is used to the limit

$$\mu_T = \frac{|\overline{\rho u'' v''}|}{|\Omega_{ij}|} = \frac{a_1 \rho k}{|\Omega_{ij}|} \quad (29)$$

This is called the SST-limitation of μ_T . SST-limitation improves significantly the behavior of the model in boundary layers that has unfavorable pressure gradient, in which cases the traditional model clearly overestimates the turbulent viscosity.

The meaning of function F_3 is to prevent an activation of the SST-limitation near the rough walls [5, 6]. Function F_3 is defined as

$$F_3 = 1 - \tanh \left[\left(\frac{150\nu}{\omega d^2} \right)^4 \right] \quad (30)$$

where d is a distance from the walls.

4 Computational Grid

The computational grid structure is depicted in Fig. 1. In the C-type grid used with FINFLO-7.2 there is one computation block, and it is divided into three blocks as used with FINF2D. Grid dimensions are 193 in I -direction and 65 in J -direction. The grid used with FINF2D is divided into three parts in a way that C-type grid is cut just after the airfoil end and replaced with two H-type blocks. The reason for the block-division with the FINF2D lies in the restricted definition of the solid surfaces.

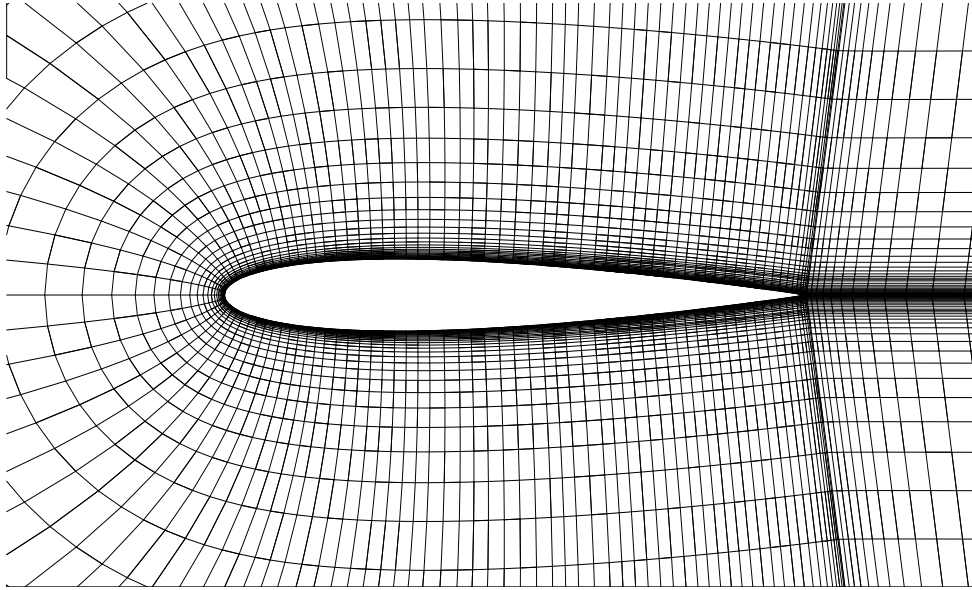


Fig. 1: Computaional grid.

5 Results

The case is calculated utilizing the $k - \varepsilon$ and the $k - \omega$ turbulence models with both codes. In addition a circulation correction at the outer boundary of the computational domain is tested with the $k - \omega$ turbulence model simulation with the FINF2D code. A third-order upwind biased discretization is used in the calculation of the convective fluxes. The angle of attack is 10 degrees and the Mach number is 0.3. Convergence histories of the lift and drag coefficient,

$\|L\|_2$ norm of a y -moment residual and a budget of turbulent kinetic energy are shown in Appendix A for the $k - \varepsilon$ model and in Appendix B for the $k - \omega$ model. It is seen that the convergence histories are different. In the FINFLO-7.2 histories a periodic solution is established indicating a small separation. That is not, however, visible in the C_f - and C_p -distributions. It should be noted that the FINFLO-7.2 solution is basically three dimensional although the case is two-dimensional. This may affect the solutions.

Drag and lift coefficients are presented in Table 1. The drag coefficients are varying a lot, as the difference between the smallest and largest value is nearly 21 %. The lift coefficients are varying by 4%. Circulation correction has a bigger influence on the drag coefficient as the code version does.

Table. 1: Drag and lift coefficients

Code	Turb. model	C_D	C_D/C_{Dmin}	C_L	C_L/C_{Lmin}
FINFLO-7.2	$k - \varepsilon$	0.019024	1.10985	1.115250	1.04189
FINF2D	$k - \varepsilon$	0.021255	1.24000	1.095614	1.02355
FINFLO-7.2	$k - \omega$	0.018036	1.05221	1.083648	1.01237
FINF2D	$k - \omega$	0.019534	1.13960	1.070401	1.00000
FINF2D*	$k - \omega$	0.017141	1.00000	1.085269	1.01389

* Circulation correction

Friction and pressure coefficients over the airfoil are shown in Figs. 2 - 5. The friction coefficient calculated utilizing the $k - \varepsilon$ turbulence model is slightly different as calculated with the different codes, but otherwise the curves are very near each other. Especially with the $k - \omega$ model both the C_f - and the C_p -distributions are practically identical. This indicates that the model is similarly implemented in both codes. However, especially the drag coefficient differs a lot, by more than 8 %. The reason for this is unknown.

The maximum values of the friction coefficient are presented in Table 2. The difference between the highest and the lowest value is 11 %, and between $k - \omega$ model simulations 4 %. The location of the stagnation point is one computational cell below the centre line of the airfoil except with FINF2D and $k - \varepsilon$ model it is two cell below the centre line.

Table. 2: Maximum values of the friction coefficient

Code	Turb. model	C_f	C_f/C_{fmin}
FINFLO-7.2	$k - \varepsilon$	0.02294	1.00000
FINF2D	$k - \varepsilon$	0.02501	1.09023
FINFLO-7.2	$k - \omega$	0.02569	1.11987
FINF2D	$k - \omega$	0.02463	1.07367

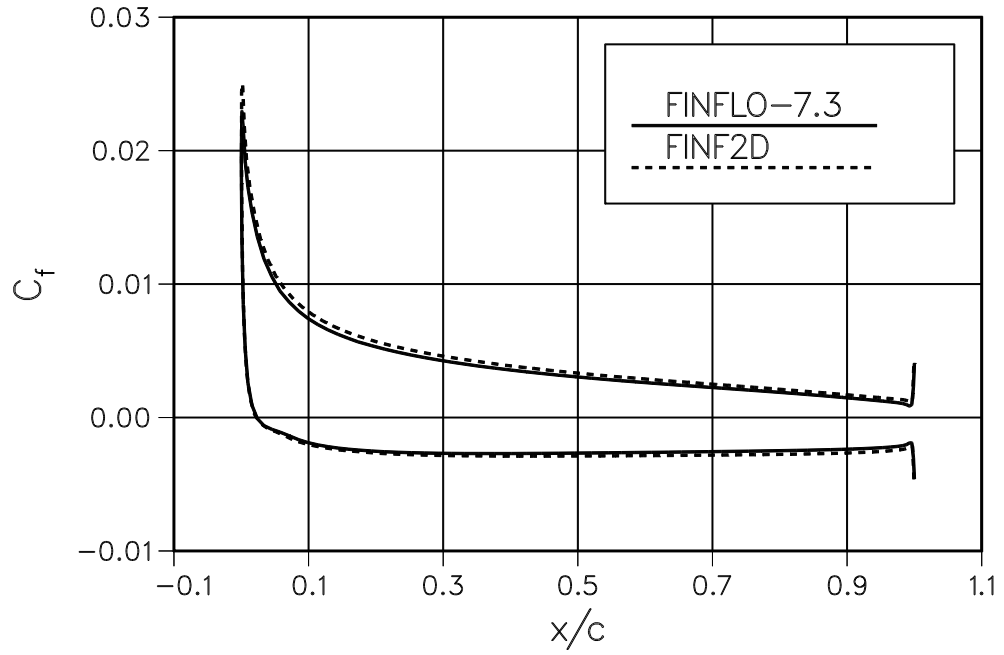


Fig. 2: Friction coefficient over the airfoil as calculated with the $k - \varepsilon$ turbulence model.

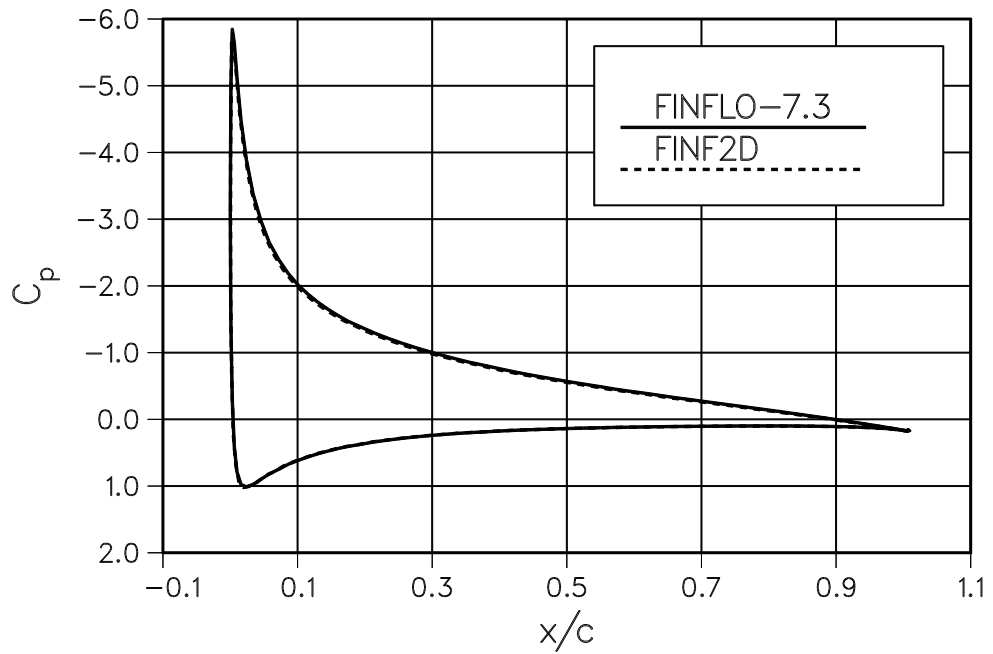


Fig. 3: Surface pressure coefficient over the airfoil as calculated with the $k - \varepsilon$ turbulence model.

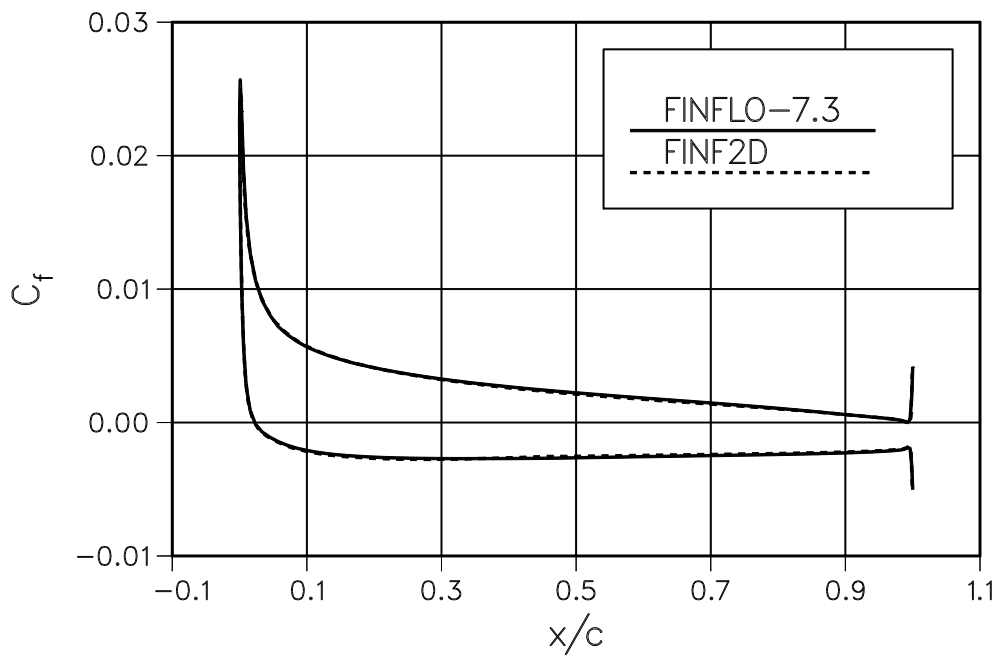


Fig. 4: Friction coefficient over the airfoil as calculated with the $k - \omega$ turbulence model.

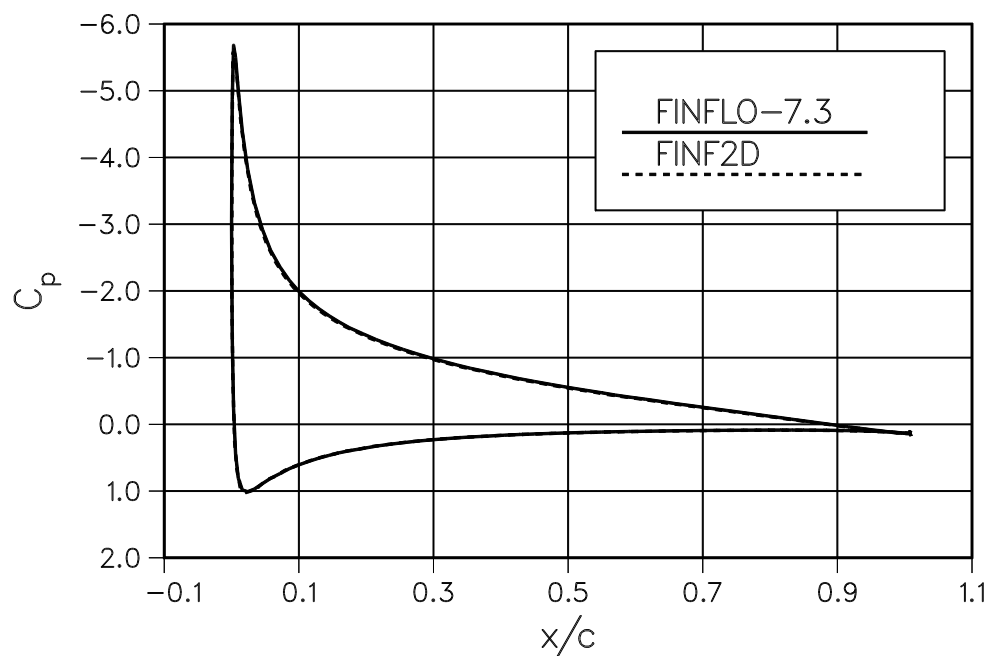


Fig. 5: Surface pressure coefficient over the airfoils calculated with the $k - \epsilon$ turbulence model.

Mach number distribution and velocity vectors are depicted in Fig. 6. The velocity vectors also show the stations of the velocity distributions shown in Figs. 7 - 10. Velocity distributions are quite close to each other. In boundary layer area with the $k - \varepsilon$ there is more difference.

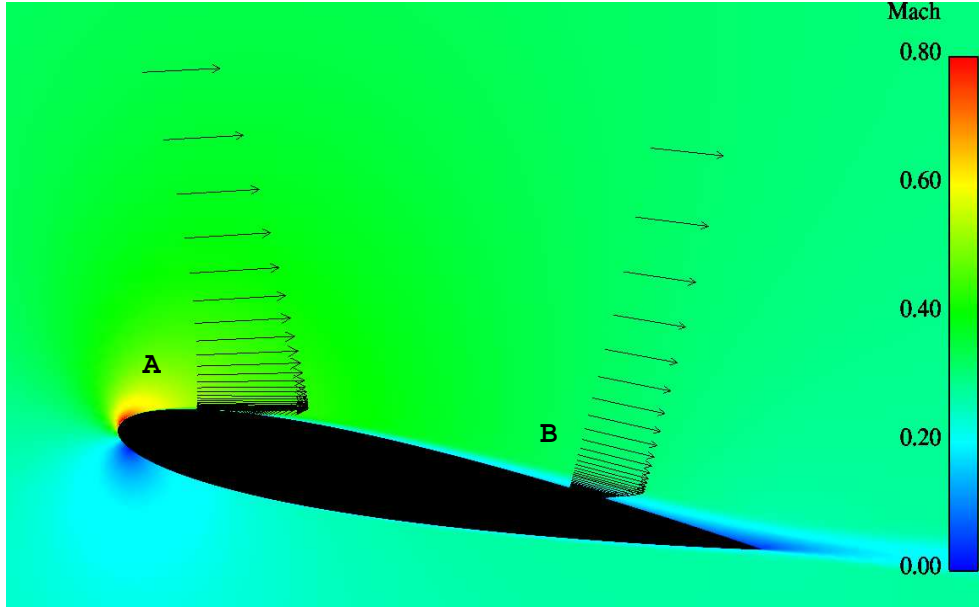


Fig. 6: Mach number distribution and velocity vectors as calculated with the FINFLO-7.2 and $k - \omega$ turbulence model.

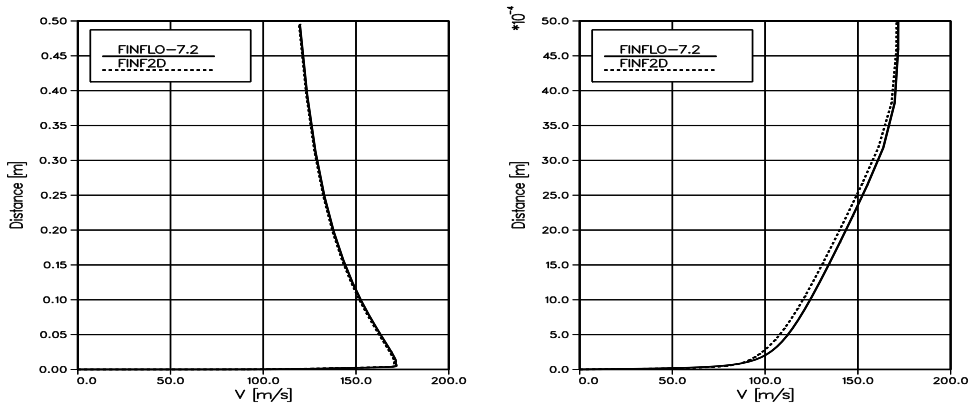


Fig. 7: Velocity distributions at station A (see Fig. 6) and velocity distributions in boundary layer at station A, as calculated with the $k - \varepsilon$ turbulence model.

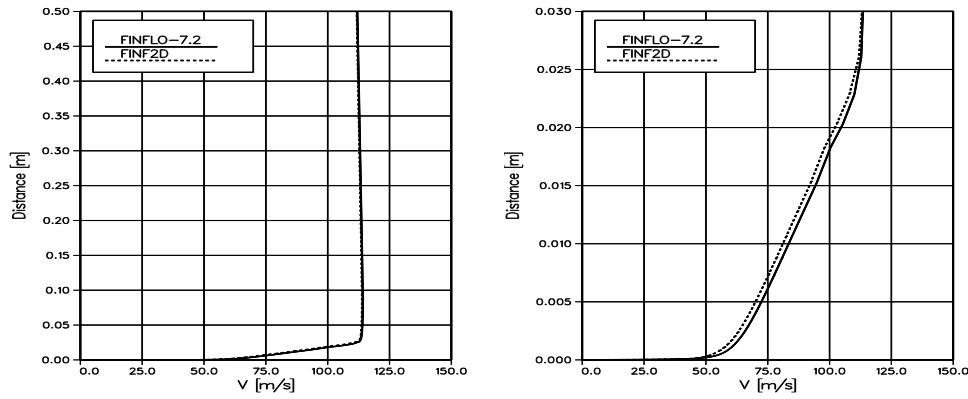


Fig. 8: Velocity distributions at station B (see Fig. 6) and velocity distributions in boundary layer at station B, as calculated with the $k - \varepsilon$ turbulence model.

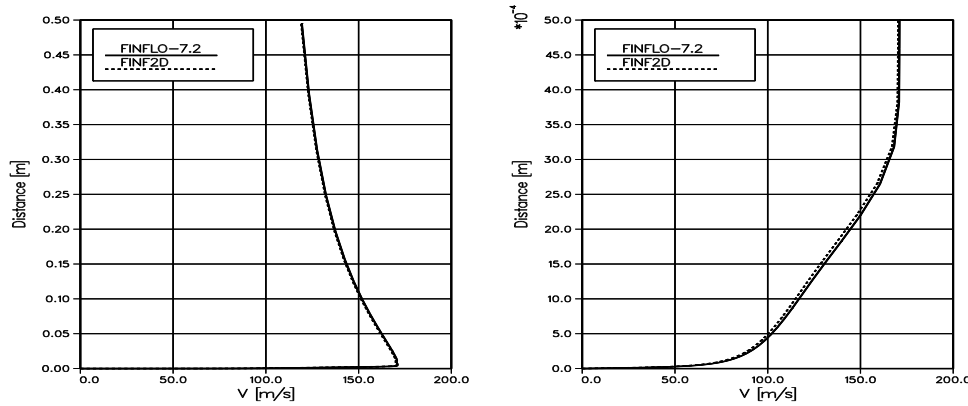


Fig. 9: Velocity distributions at station A (see Fig. 6) and velocity distributions in boundary layer at station A, as calculated with the $k - \varepsilon$ turbulence model.

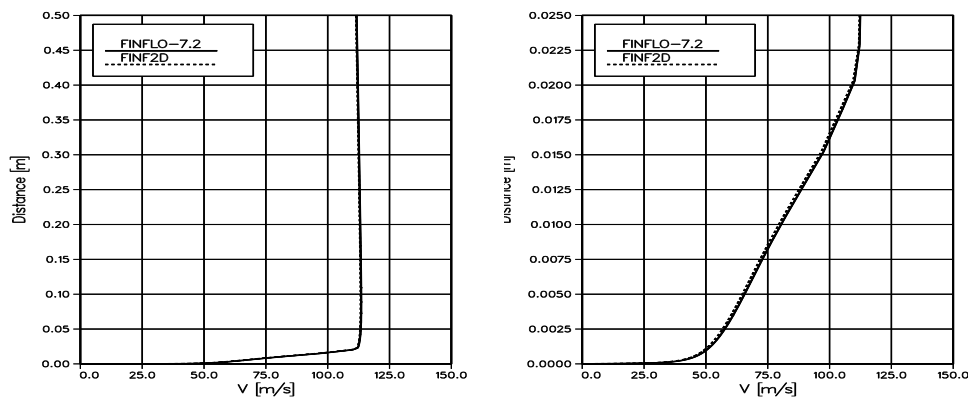


Fig. 10: Velocity distributions at station B (see Fig. 6) and velocity distributions in boundary layer at station B, as calculated with the $k - \omega$ turbulence model.

6 Discussion

The flow around the the NACA 0012 airfoil was simulated numerically with two different, but basicly similar flow solvers, utilizing $k - \varepsilon$ and $k - \omega$ turbulence models.

Drag and lift coefficient are unequal between the turbulence models and solver codes. The difference is nearly 18 % at the largest. With the $k - \omega$ model, where the simulation was considered to be more adequate, the drag value differs by 8.3 %. The difference in the lift coefficient is 1.2 %.

Friction and pressure coefficients are very near each other between the solvers. The largest difference is between the friction coefficient calculated with the $k - \varepsilon$ model. In that case the friction coefficient curve calculated with FINF2D solver changed considerably between 30 000 and 50 000 cycles although the convergence histories does not indicate nothing special there. Since, the C_f - and C_p -distributions with the $k - \omega$ model are so close to each other, it is concluded that the turbulence models are similar in both codes. The differences in the force coefficients are caused by some unknown factor.

References

- [1] Chien, K.-Y., “Predictions of channel and boundary-layer flows with a low-Reynolds-number turbulence model,” *AIAA Journal*, Vol. 20, No. 1, 1982, pp. 33–38.
- [2] *FINFLO User Manual version 2.2*, 1997.
- [3] Menter, F., “Zonal two equation $k - \omega$ turbulence models for aerodynamic flows,” in *24th AIAA Fluid Dynamics Conference*, AIAA, 1993. AIAA Paper 93–2906.
- [4] Menter, F., “Two-equation eddy-viscosity turbulence models for engineering applications,” *AIAA Journal*, Vol. 32, No. 8, 1994, pp. 1598–1605.
- [5] Hellsten, A. and Laine, S., “Extension of the $k - \omega$ Shear-Stress Transport Turbulence Model for Rough-Wall Flows,” *AIAA Journal*, Vol. 36, No. 9, 1998, pp. 1728–1729.
- [6] Hellsten, A. and Laine, S., “Extension of the $k - \omega$ -SST Turbulence Model for Flows over Rough Surfaces,” in *1997 AIAA Atmospheric Flight Mechanics Conference*, (New Orleans, Louisiana), pp. 252–260, Aug 1997. AIAA Paper 97–3577–CP.

A Convergence histories of the $k-\varepsilon$ turbulence model

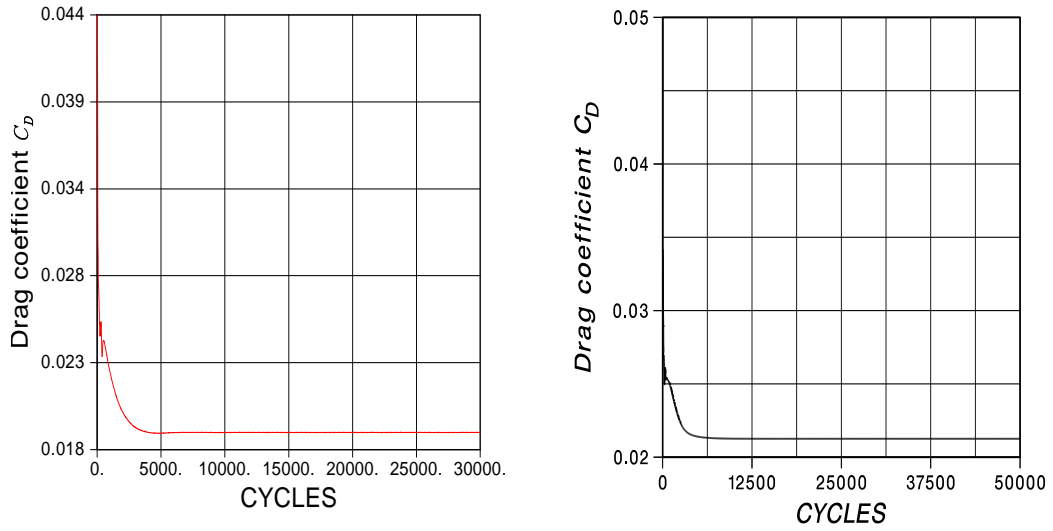


Fig. 11: Convergence history of drag coefficient as simulated with the FINFLO-7.2 (left) and the FINF2D (right).

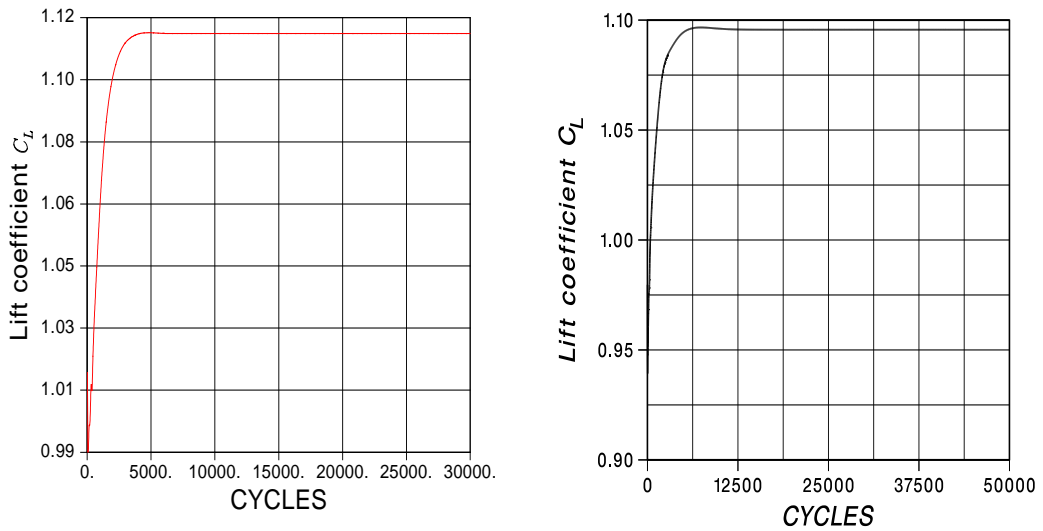


Fig. 12: Convergence history of lift coefficient as simulated with the FINFLO-7.2 (left) and the FINF2D (right).

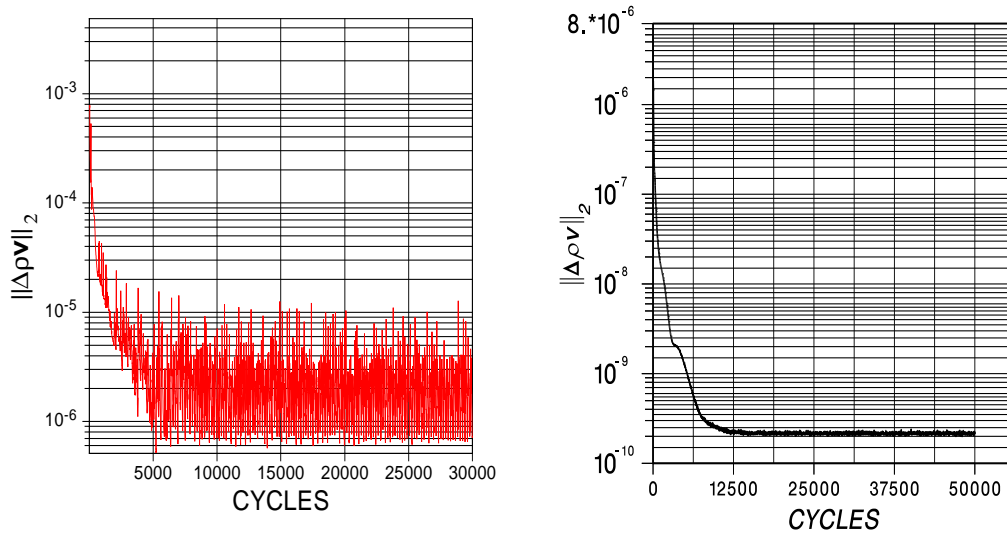


Fig. 13: Convergence history of the $\|L\|_2$ norm of the y -moment residual as simulated with the FINFLO-7.2 (left) and the FINF2D (right).

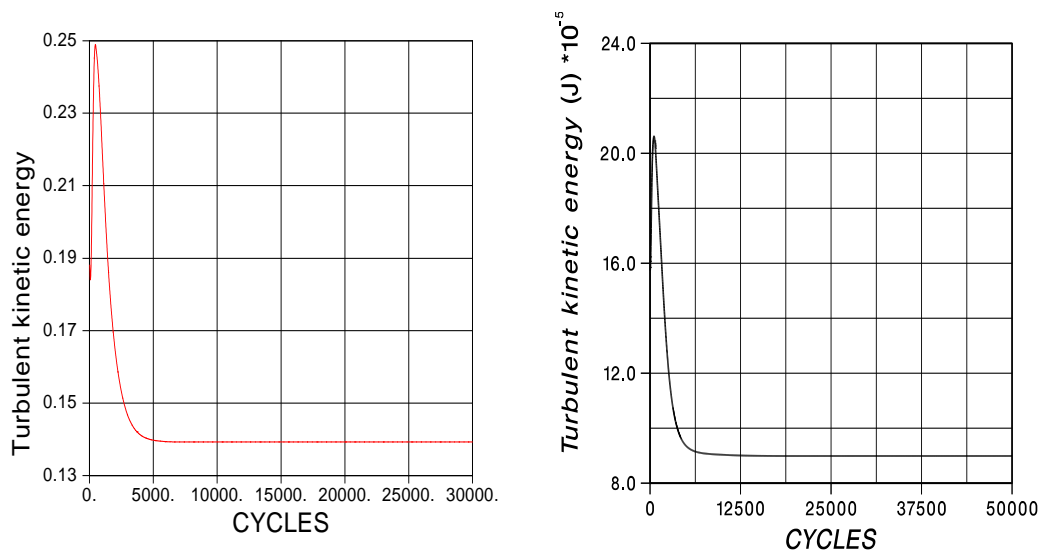


Fig. 14: Convergence history of the turbulent kinetic energy as simulated with the FINFLO-7.2 (left) and the FINF2D (right).

B Convergence histories of the $k - \omega$ turbulence model

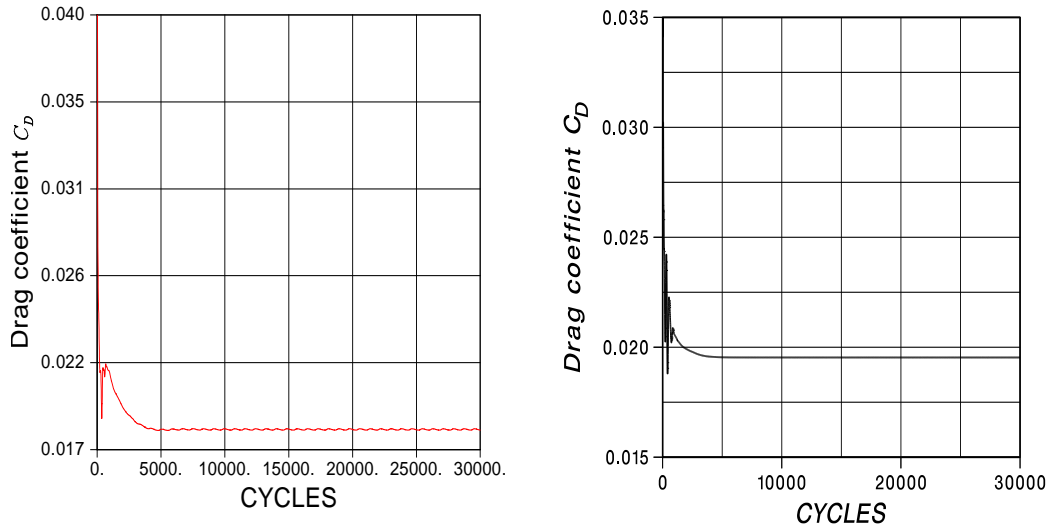


Fig. 15: Convergence history of drag coefficient as simulated with the FINFLO-7.2 (left) and the FINF2D (right).

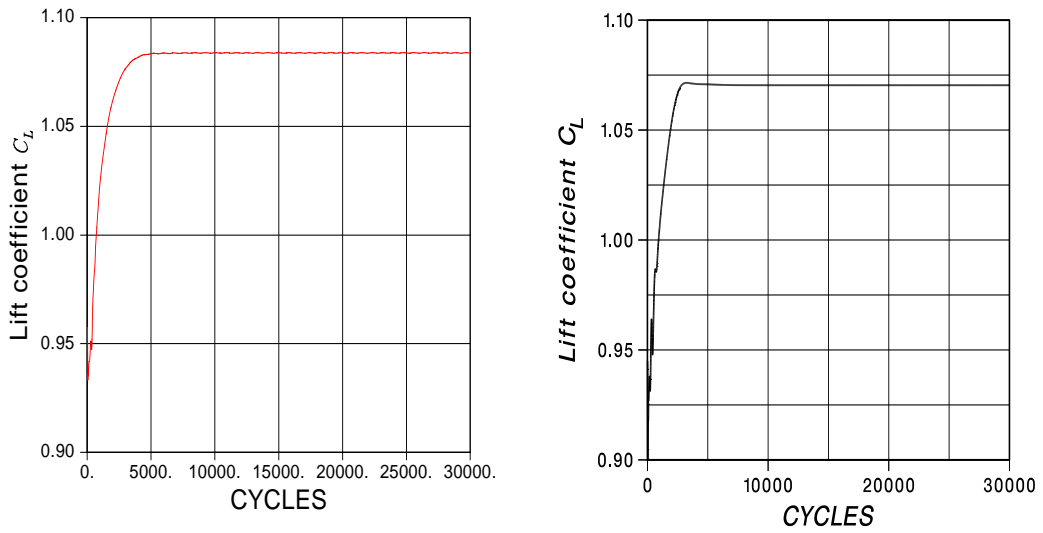


Fig. 16: Convergence history of lift coefficient as simulated with the FINFLO-7.2 (left) and the FINF2D (right).

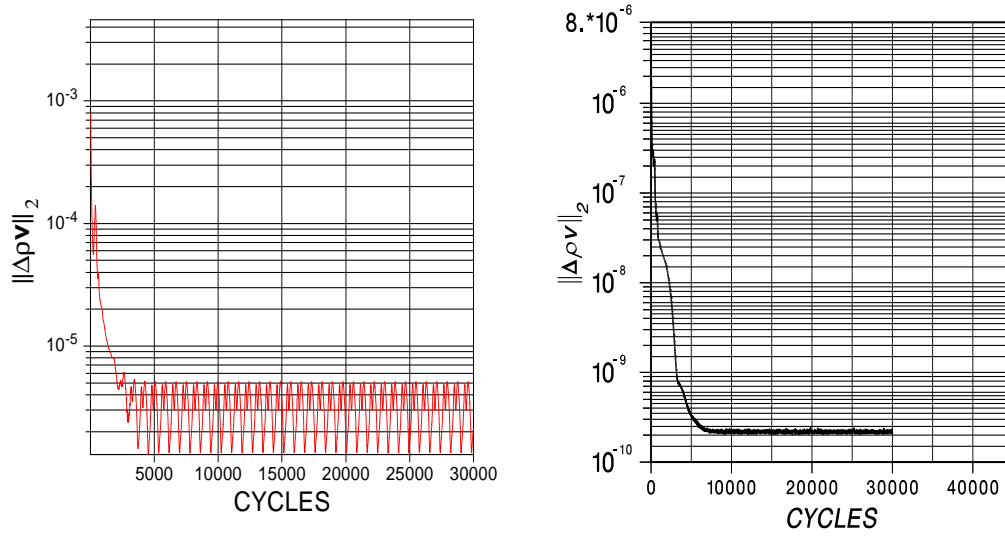


Fig. 17: Convergence history of the $\|L\|_2$ norm of the y -moment residual as simulated with the FINFLO-7.2 (left) and the FINF2D (right).

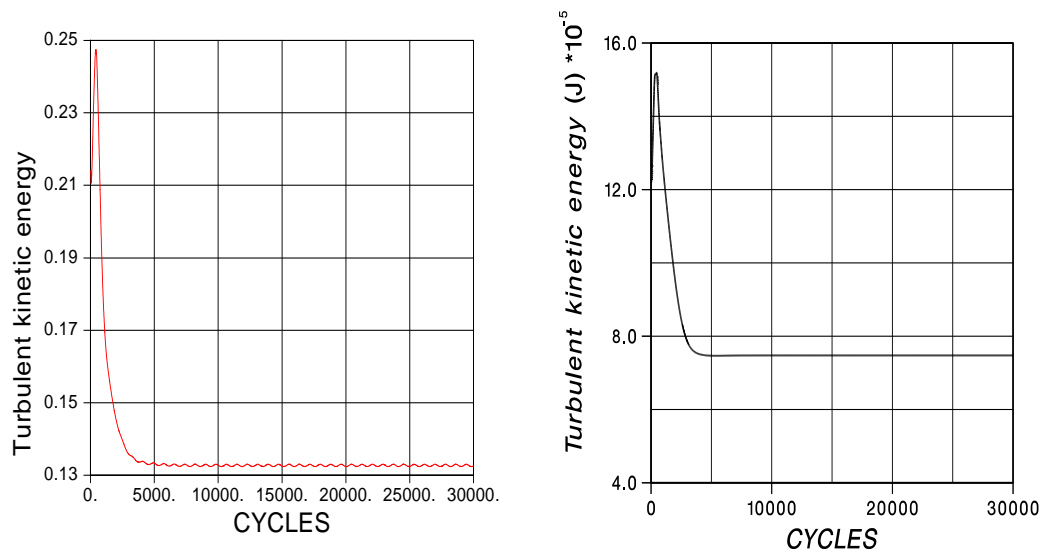


Fig. 18: Convergence history of the turbulent kinetic energy as simulated with the FINFLO-7.2 (left) and the FINF2D (right).